

ELECTRICAL DISCHARGE IN A SUPERSONIC AIR FLOW

V. I. ALFEROV and A. S. BUSHMIN

Submitted to JETP editor December 29, 1962

J. Exptl. Theoret. Phys. (U.S.S.R.) 44, 1775-1779 (June, 1963)

The results are given of an investigation of an electrical discharge in a moving gas for Mach numbers  $M = 0-4.5$ . The discharge was investigated using two electric-circuit variants: 1) with a ballast resistor, and 2) with a shunted ballast resistor. In the first case the discharge had a falling current-voltage characteristic. It was distinguished by a high voltage of the electrodes during the discharge. In the second case the discharge was similar to the breakdown of a discharge gap and was characterized by a pre-breakdown glow and increase of the breakdown voltage with increase of the Mach number  $M$  of the gas flow, other conditions being equal.

THERE is great interest at present in the study of the interaction of an electrical discharge with a gas flowing at a high velocity. Such studies are relevant to the heating of a supersonic gas flow by an electrical discharge, problems in the development of various magnetohydrodynamic generators, etc.

1. DESCRIPTION OF THE EXPERIMENT

The electrical discharge was investigated in a closed wind tunnel with two supersonic ejector pumps. The gas flow Mach number  $M$  was varied within the limits 0-4.5 by using interchangeable nozzles. The velocity field at the exit from a nozzle was highly uniform.

Investigations were carried out for  $M = 0.0, 0.5, 1.5, 3.0$  and  $4.5$ , and gas densities  $\rho = 0.135, 0.270, 0.405, 0.540 \text{ kg/m}^3$ . Since the stagnation temperature was constant ( $T_0 \approx 283^\circ\text{K}$ ) and the static temperature varied with the  $M$  number of the gas flow, the static pressure was varied in order to have the same gas density at various  $M$  numbers. The values of the static pressures and static temperatures are listed in the table for the  $M$  numbers given above.

The experimental arrangement is shown in Fig. 1. Cylindrical (5 mm diameter) molybdenum electrodes 4 with rounded ends were placed in the

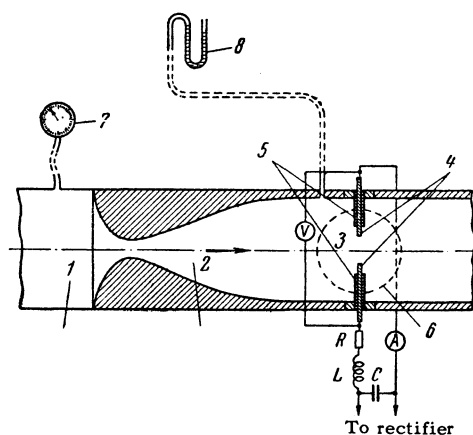


FIG. 1. Experimental arrangement. 1) Fore-chamber; 2) Laval nozzle; 3) working region; 4) electrodes; 5) teflon fairings; 6) optical-glass window; 7) manometer for measuring the fore-chamber pressure; 8) manometer for measuring the static pressure.

working part of the apparatus 3. The nonworking parts of the electrodes were covered with rhomboidal fairings 5 made of teflon. It should be noted that the electrode erosion during the experiments was negligible.

The streamline flow field in the absence of a discharge was photographed by the direct-shadow method. An actual flow picture is shown in Fig. 2.

M	Pstat, mm Hg				Tstat, °K
	$\rho = 0.135$	$\rho = 0.270$	$\rho = 0.405$	$\rho = 0.540$	
0,0	84	168	252	336	283
0,5	80	160	240	320	281
1,5	57,5	115	173	230	195
3,0	30	60	90	120	101
4,5	16,6	—	—	—	57



FIG. 2. Photograph of flow past the electrodes:  $M = 3.0$ ;  $l = 15$  mm;  $p_{\text{stat}} = 60$  mm Hg.

A special automatic device, located outside the tunnel, made it possible to move the electrodes during an experiment. Investigations were carried out for various distances  $l$  between the electrodes: 10, 15, 20 and 25 mm.

The electrical discharge was fed with dc from a single-phase rectifier using gas-filled rectifier tubes of VG-237 type, connected in a bridge circuit. The operating regime of the rectifier was controlled with an ammeter. The average value of the current in the electrode circuit was kept at  $I_{\text{av}} = 2.5$  A. The voltage between the electrodes was measured with an electrostatic kilovoltmeter of S96 type. Investigations were carried out using two variants of electric-circuit operation. In the first, the electric circuit included a stabilizing ballast resistor. In this case the circuit parameters were: resistance  $R = 950 \Omega$ , inductance  $L = 7.4 \times 10^{-3}$  H, capacitance  $C = 15 \times 10^{-6}$  F. In the second variant the ballast resistor was shunted. The circuit in this case had the following parameters:  $R = 0.28 \Omega$ ,  $L = 24 \times 10^{-6}$  H,  $C = 15 \times 10^{-6}$  F. In each case tests were carried out both with and without gas flow.

In the first variant the discharge current was recorded in the absence of gas flow with an oscillograph MPO-2 on a film moving at 500 mm/sec using a loop with a natural frequency of 5000 cps. In the presence of gas flow the current-voltage characteristics were recorded, the current being measured oscillographically on a film moving at 1000 mm/sec, and the form of the discharge was photographed with an AKS-2 camera.

In the second variant the breakdown voltage across a discharge gap was measured with an S96 kilovoltmeter under various conditions, and the form of the discharge was photographed with a Zorkii-6 camera.

## 2. RESULTS OF INVESTIGATIONS AND DISCUSSION

a) First Variant (with a ballast resistor). When this variant was used, in the absence of gas flow the discharge was in the form of a series of flashes, but in the presence of gas flow the discharge exhibited high stability which increased with increase of the flow velocity. This indicates that the discharge gap resistance rises considerably in the presence of gas flow.

The current-voltage characteristics of the discharge for  $M = 3.0$ , static pressures  $p_{\text{stat}} = 30, 60$  and  $90$  mm Hg, and interelectrode distances  $l = 10, 15$  and  $20$  mm, are given in Fig. 3. These characteristics are of falling type, indicative of a stable arc discharge.

Photographs of the discharge for various  $M$  numbers and certain values of static pressures and inter-electrode distances are given in Fig. 4.

All the photographs show a luminous trail behind the electrodes, in which there are several bands bounded by an outer luminous zone of greatest brightness. Depending on the gas flow velocity the form and number of the inner zones varies from one to three. Thus, for example, Fig. 4a shows the form of the discharge for a gas flow with  $M = 0.5$ . In this case there is one clearly defined inner zone with a weak glow. On increase of the flow velocity to  $M = 1.5$  (Fig. 4b) an unstable inner band appears with the trail having bright and dark parts behind the arc. On further increase of the gas velocity ( $M = 3.0$ ) a third band in the form of an inner channel appears and the general form of the discharge becomes more stable. Finally for  $M = 4.5$ , Fig. 4d shows a fully stable form; a fourth

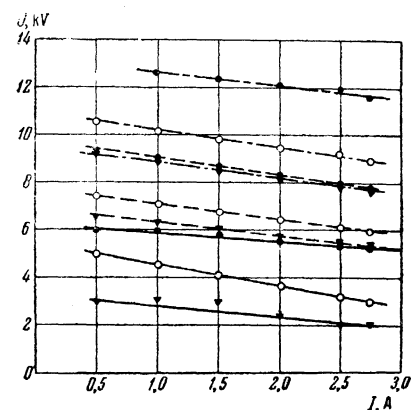


FIG. 3. Current-voltage characteristics for discharges with  $M = 3.0$ : continuous curve represents  $p_{\text{stat}} = 30$  mm Hg, dashed curve -  $p_{\text{stat}} = 60$  mm Hg, chain curve -  $p_{\text{stat}} = 90$  mm Hg;  $\nabla$  -  $l = 10$  mm;  $\circ$  -  $l = 15$  mm;  $\bullet$  -  $l = 20$  mm.

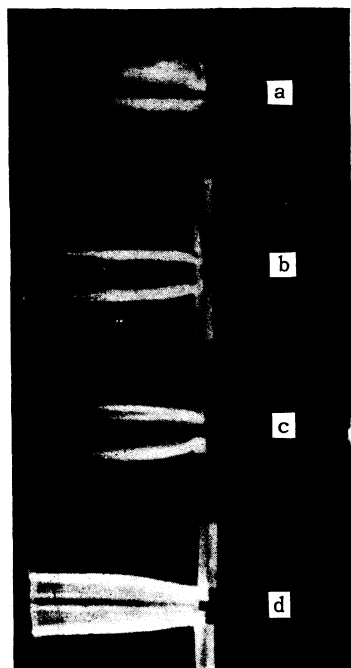


FIG. 4. Form of the electrical discharge in the presence of a ballast resistor: a)  $M = 0.5$ ,  $l = 10$  mm,  $p_{\text{stat}} = 320$  mm Hg,  $U_{\text{av}} = 5$  kV,  $I_{\text{av}} = 2.5$  A; b)  $M = 1.5$ ,  $l = 20$  mm,  $p_{\text{stat}} = 117$  mm Hg,  $U_{\text{av}} = 8$  kV,  $I_{\text{av}} = 2.5$  A; c)  $M = 3.0$ ,  $l = 10$  mm,  $p_{\text{stat}} = 30$  mm Hg,  $U_{\text{av}} = 3.2$  kV,  $I_{\text{av}} = 2.5$  A; d)  $M = 4.5$ ,  $l = 10$  mm,  $p_{\text{stat}} = 16.6$  mm Hg,  $U_{\text{av}} = 2$  kV,  $I_{\text{av}} = 2.5$  A.

zone is formed in the form of a bright luminous layer which defines the inner channel.

In the latter case there is a certain symmetry: the inner channel with two luminous zones, compressed between hotter and denser gas, lies within an outer channel which also has two luminous zones.

A detailed investigation of the physical properties of the discharge zones is at present being carried out. One may expect that neutral atoms of the electrode materials predominate in the bright luminous bands, as is usually observed in arcs, and that excited molecules are present in the space between the bands.

A channel joining the two electrodes is seen in Fig. 4b for  $M = 1.5$ . This channel was also observed for other  $M$  numbers but it was of a pulse nature and therefore was not always recorded. Oscillograms of the current are given in Figs. 5 and 6. Figure 5b shows an oscillogram characteristic of an arc discharge. Such oscillograms were observed only for  $M = 0$  and 4.5, inter-electrode distances not greater than 15 mm, and gas densities not greater than  $0.27$  g/m<sup>3</sup>. In all the remaining cases the oscillograms were similar to those shown in Fig. 5a and 5c.

Oscillograms of the current showed that the

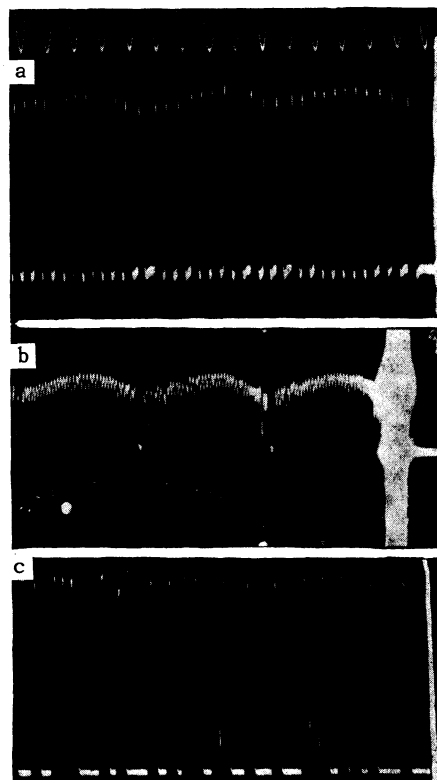


FIG. 5. Oscillograms of the current in the presence of gas flow. Film moving at 1000 mm/sec. Current pulse duration  $\tau = 0.7 \times 10^{-3}$  sec. Frequency marks at 500 cps. a)  $M = 1.5$ ,  $l = 15$  mm,  $p_{\text{stat}} = 117$  mm Hg, current amplitude 7.5 A; b)  $M = 3.0$ ,  $l = 10$  mm,  $p_{\text{stat}} = 30$  mm Hg, current amplitude 3.5 A; c)  $M = 3.0$ ,  $l = 15$  mm,  $p_{\text{stat}} = 60$  mm Hg, current amplitude 7 A.

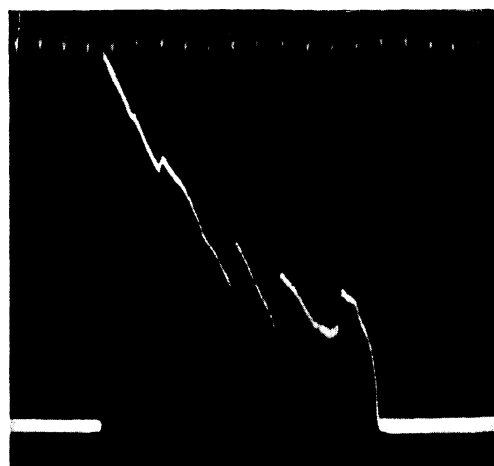


FIG. 6. Current oscillogram in the absence of gas flow:  $l = 10$  mm,  $p_{\text{stat}} = 168$  mm Hg, frequency marks at  $f = 500$  cps. Current pulse duration  $\tau = 22 \times 10^{-3}$  sec. Film moving at 500 mm/sec.

current amplitude  $I = U_{\text{br}}/R_{\text{ball}}$  depends on the  $M$  number in the same way as the breakdown voltage  $U_{\text{br}}$ ;  $R_{\text{ball}}$  is the ballast resistance. The re-

sults of a study of the breakdown voltage are reported below. Comparison of the current oscillograms without (Fig. 6) and with air flow (Fig. 5) shows that the gas flow reduces the duration of current pulses considerably. Thus in the case of a current oscillogram for  $p_{\text{stat}} = 768$  mm Hg and  $l = 10$  mm without air flow (Fig. 6) the pulse duration is  $\tau \approx 22 \times 10^{-3}$  sec, while for  $p_{\text{stat}} = 117$  mm Hg,  $l = 15$  mm and  $M = 1.5$  (Fig. 5a) the pulse duration is  $\tau \approx 0.7 \times 10^{-3}$  sec. The conditions under which these two oscillograms were recorded differed not only by the presence of air flow, but also in other parameters, but it was established during these experiments that the inter-electrode distance, gas density, and the  $M$  number do not affect greatly the duration of the current pulse. It is possible to explain the reduction of the current pulse duration in the presence of gas flow by the faster removal of the ionization products and the faster return of the gap and electrode temperature to the ambient temperature.

b) Second Variant (without a ballast resistor).

The form of the discharge obtained in the second variant is shown in Fig. 7. In this case the discharge represents a breakdown of the discharge gap. Later the various stages of breakdown development will be recorded by high-speed photography. Visual observations showed the following difference in the development of breakdown with and without air flow. In the presence of air flow at near-breakdown voltage a violet glow appears between the electrodes. On increase of the voltage the dimensions and intensity of the glow region increase (the positions of the shock waves are seen clearly in the form of dark lines against the glow background) and finally breakdown occurs. During breakdown the region of the brightest glow coincides with the position of the shock wave (cf. Figs. 2 and 7).

The right-hand parts of the Paschen curves for various  $M$  numbers are given in Fig. 8. In plotting these curves the method of least squares was employed. Averaging was done for points which were arithmetic means of five measurements. These points are shown in the figure. The considerable scatter of points in the absence of gas flow may be due to difficulties connected with maintaining a fixed gas density by means of ejector fans.

From Fig. 8 it follows that, other conditions being equal, with increase of the  $M$  number of the gas the breakdown voltage increases, beginning from certain values of the gas density and inter-electrode distance. We may assume that a certain delay in the onset of breakdown and the rise of  $U_{\text{br}}$  with

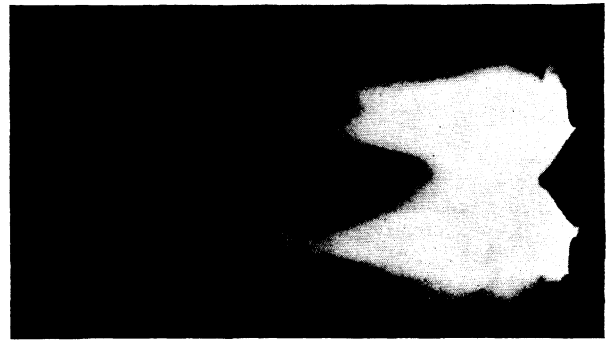


FIG. 7. Photograph of a breakdown at  $M = 3.0$ ,  $l = 15$  mm,  $p_{\text{stat}} = 60$  mm Hg.

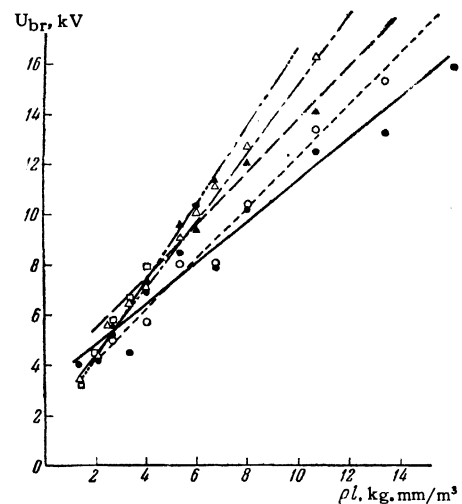


FIG. 8. Right-hand parts of the Paschen curves: continuous curve and  $\bullet$  for  $M = 0.0$ ; dashed curve and  $\circ$  for  $M = 0.5$ ; dashed curve and  $\blacktriangle$  for  $M = 1.5$ ; chain curve and  $\Delta$  for  $M = 3.0$ ; chain curve and  $\square$  for  $M = 4.5$ .

increase of  $M$  are both due to the same cause. The most likely explanation is as follows: gas flow removes ions from avalanches which have not yet become streamers; this leads to the formation of a space charge which may impede propagation of electron avalanches.

Thus during these experiments two types of electrical discharge were observed in supersonic air flow. The discharge using a circuit with a ballast resistor has a falling current-voltage characteristic and is distinguished by a high voltage at the electrodes during arcing. The characteristic features of the discharge obtained using a circuit without a ballast resistor (the breakdown discharge) are the appearance of a violet glow before the beginning of breakdown and increase of the breakdown voltage with increase of the  $M$  number, other conditions being equal.

The authors thank B. V. Kalachev and A. V. Polyakova for taking part in the experiments and discussing the results.

---

<sup>1</sup>Alferov, Ryabinkov, and Petrov, *Issledovanie vysokovol'tnogo élektricheskogo razryada v sverkhzvukovom potoke* (Investigation of High-voltage Electrical Discharge in Supersonic Flow), *Trudy, Moscow Physico-technical Inst.*, No. 4 (1959).

<sup>2</sup>J. M. Meek and J. D. Craggs, *Electrical Break-down of Gases*, Oxford Univ. Press, 1953.

<sup>3</sup>Edels, Shaw, and Whittaker, *Proc. Fifth Intern. Conf. on Ionization Phenomena in Gases*, Amsterdam, North-Holland Publ. Co. 1962.

Translated by A. Tybulewicz  
281